

Spin Polarization of Photoelectrons from Topological Insulators

Cheol-Hwan Park and Steven G. Louie*

Department of Physics, University of California at Berkeley, Berkeley, California 94720
Materials Sciences Division, Lawrence Berkeley National Laboratory, Berkeley, California 94720

(Dated: June 10, 2018)

We show that the degree of spin polarization of photoelectrons from the surface states of topological insulators is 100 % if fully-polarized light is used as in typical photoemission measurements, and hence can be significantly *higher* than that of the initial state. Further, the spin orientation of these photoelectrons in general can also be very different from that of the initial surface state and is controlled by the photon polarization; a rich set of predicted phenomena have recently been confirmed by spin- and angle-resolved photoemission experiments.

Three-dimensional topological insulators (TIs) are strong spin-orbit interaction materials characterized by a bulk electronic gap and metallic topological surface state (TSS) bands with linear energy dispersions [1–3]. The predicted linear energy dispersion of the TSSs in TIs were first observed in angle-resolved photoemission spectroscopy (ARPES) measurements [4]. TIs are considered to be a promising candidate for spintronic devices because of their spin-momentum locking [5–7]. Aspects of the spin distribution of the TSSs in TIs have been measured by spin-resolved ARPES experiments [8–13].

Because the spin orientation of the photoelectron in the specific conditions used in previous spin-resolved ARPES studies agreed with the expected picture of the spin distribution of the TSS electrons in TIs [Fig. 1(a)], photoemission matrix element effects were neglected in analyzing the spin polarization of the photoelectrons. (On the other hand, matrix element effects have been used in analyzing the circular dichroism of the TSS electrons in a TI [14–17].)

Here, we find that the degree of spin polarization of photo-ejected electrons as defined in typical measurements with fully-polarized light is significantly higher (can in principle be 100%) than that of the TSSs ($\sim 50\%$ for Bi_2Se_3 and Bi_2Te_3 according to first-principles calculations [6]), explaining the origin of high values of the measured degree of polarization (75% and $> 85\%$ in Pan *et al.* [12] and Jozwiak *et al.* [13], respectively, from experiments on Bi_2Se_3). Moreover, using the symmetries of the TI surface, we find that electron-photon interactions can completely alter the spin orientation of the photo-ejected electrons relative to that of the initial state and that the spin orientation of these photoelectrons can be controlled via light polarization tuning. For linearly polarized light, the detected spin orientation is significantly altered except for the specific case of the wavevector \mathbf{k} of an initial state being parallel to the in-plane component of the light polarization $\hat{\epsilon}$. For \mathbf{k} orthogonal to $\hat{\epsilon}$, the two spins are predicted to be antiparallel to each other. Moreover, for in-plane circularly polarized light, the spins of the photoelectrons are oriented either completely parallel or completely antiparallel to the surface normal depending on the handedness of the circular polarization.

The measured degree of spin polarization is defined through the relation

$$P_{\max} = \max_{\{\hat{t}\}} \frac{I_{\hat{t}} - I_{-\hat{t}}}{I_{\hat{t}} + I_{-\hat{t}}}, \quad (1)$$

where $I_{\hat{t}}$ and $I_{-\hat{t}}$ are the intensities for the electron spin being aligned and anti-aligned with \hat{t} , respectively. The unit vector $\hat{t} = \hat{t}_{\max}$ which maximizes Eq. (1) defines the direction of the electron spin polarization. Hsieh *et al.* [9] reported in-plane P_{\max} [i. e., restricting \hat{t} in Eq. (1) in the surface plane] to be 20% for photoelectrons from the TSSs of Bi_2Se_3 , Souma *et al.* [10] and Xu *et al.* [11] reported 60% for those of Bi_2Te_3 , and Pan *et al.* [12] and Jozwiak *et al.* [13] reported 75% and $> 85\%$, respectively, for those of Bi_2Se_3 . On the other hand, the degree of in-plane spin polarization of the TSSs for both Bi_2Se_3 and Bi_2Te_3 obtained from first-principles calculations is $\sim 50\%$ [6]. It is puzzling that the measured spin polarization of the photoelectrons [12, 13] can be significantly *higher* than that of the corresponding TSS obtained from theory [6]. Due to, e. g., spin-independent background signals, the measured degree of spin polarization is expected to always be lower than that from calculation.

We find that the degree of spin polarization of photoelectrons from the TSSs of a TI is 100%. To show this, we start from the general expression for photocurrent from a detector (that selects a specific three-dimensional wavevector and hence a specific energy) with the spin quantization axis aligned with \hat{t} :

$$I_{\hat{t}} \propto \left| \sum_{\{f|E_f=E_i+h\nu\}} \langle \hat{t}, \mathbf{R}_D | f \rangle \langle f | H^{\text{int}} | i \rangle \right|^2, \quad (2)$$

where $|i\rangle$ is the initial TSS, $|f\rangle$ the photo-excited state, E_i and E_f their respective energies, $h\nu$ the photon energy, and H^{int} the light-matter interaction Hamiltonian connecting the two states. State $|\hat{t}, \mathbf{R}_D\rangle$ is the detected state: (i) its spin part is the eigenstate of $\mathbf{s} \cdot \hat{t}$ with eigenvalue $+1$ (\mathbf{s} is the Pauli matrix vector for spin half) and (ii) its spatial part is localized at \mathbf{R}_D , where the detec-

tor is, far away from the sample surface. (Note that \mathbf{R}_D is on the trajectory of the final-state wavepacket.) We dropped the obvious prefactor $\delta(E - E_i - h\nu)$ in front of the right hand side of Eq. (2) due to the energy-resolving detector which collects electrons with energy E . A formal derivation of Eq. (2) is reserved for interested readers [18]. Here we discuss the physical meaning of Eq. (2). First, we note that the detector reads spin character of the photo-excited state at \mathbf{R}_D ; hence, the near-surface part of the wavefunction affects the measured spin only indirectly through the matrix element $\langle f | H^{\text{int}} | i \rangle$. Second, a summation of the transition amplitude over degenerate photo-excited states $|f\rangle$'s is necessary because, even in principle, we cannot tell which $|f\rangle$ is involved in the detection [19].

If we denote

$$|f'\rangle = \sum_{\{f|E_f=E_i+h\nu\}} |f\rangle \langle f | H^{\text{int}} | i \rangle, \quad (3)$$

then we may rewrite Eq. (2) as

$$I_{\hat{t}} \propto |\langle \hat{t}, \mathbf{R}_D | f' \rangle|^2. \quad (4)$$

Since the measurement is performed at \mathbf{R}_D , far away from the sample where $|f\rangle$'s are eigenstates of the free-electron Hamiltonian, the Bloch periodic part of the state $|f'\rangle$ can be regarded as a position-independent two-element spinor in evaluating $I_{\hat{t}}$ by Eq. (4). Then, from basic spin physics, we always can find a vector \hat{t}' satisfying $|f'\rangle$ being the eigenstate of $\mathbf{s} \cdot \hat{t}'$ with eigenvalue $+1$ and the eigenstate of $\mathbf{s} \cdot (-\hat{t}')$ with eigenvalue -1 . Obviously $I_{\hat{t}'} \neq 0$ and $I_{-\hat{t}'} = 0$ for this particular orientation and we have $P_{\text{max}} = 100\%$ from Eq. (1), i. e., the degree of spin polarization of photo-ejected electrons is always 100% regardless of that of the initial electronic state.

An important ingredient that led us to this result is that the initial TSS electronic state $|i\rangle$ is not degenerate. If it is, a hole will be left in one of those *different* degenerate TSSs $|i\rangle$'s after photodetection. Therefore, we can distinguish in principle which initial TSS is involved in the measurement; the detection probability amplitude corresponding to each $|i\rangle$ should be first squared and then summed, and not the other way round [19], i. e., the photocurrent $I_{\hat{t}}$ will be the sum of contributions coming from all the degenerate initial TSSs $|i\rangle$'s. If this happens, $P_{\text{max}} \neq 100\%$. The simplest example is, for a normal spin-degenerate material, $I_{\hat{t}}$ and $I_{-\hat{t}}$ will always be the same regardless of the choice \hat{t} , making $P_{\text{max}} = 0$.

Now we apply this general consideration to the case of the TSSs of a TI. According to recent *ab initio* calculations [6], the averaged degree of spin polarization of the TSSs,

$$P_{\text{ave}}^{\text{TSS}} = |\langle \psi(n, \mathbf{k}) | \mathbf{s} | \psi(n, \mathbf{k}) \rangle|, \quad (5)$$

where $|\psi(n, \mathbf{k})\rangle$ is the two-component spinor wavefunction, is roughly 50%. Because $|\psi(n, \mathbf{k})\rangle$ is not an eigenstate of a spin operator $\hat{t} \cdot \mathbf{s}$ for any \hat{t} , the degree of spin polarization for the TSSs had to be defined as an averaged quantity. On the contrary, the degree of spin polarization of the photoelectrons P_{max} [Eq. (1)] is 100% and that is so even if we take into account the imaginary part of the self energies of the involved electronic states because the detector probes the spin character (of the photoexcited states) at \mathbf{R}_D instead of taking its average over the entire space. If the imaginary part of the initial-state self energy is considered, the condition that “the initial electronic state is not degenerate” is naturally modified to “there are no other initial electronic states in the energy window within the width of the imaginary part of the initial-state self energy.”

This result tells us that a direct comparison between P_{max} [Eq. (1)] and $P_{\text{ave}}^{\text{TSS}}$ [Eq. (5)] is not meaningful, and solves the apparent puzzle that the former from experiments [12, 13] is higher than the latter from theory ($\sim 50\%$) [6]. Although the predicted degree of spin polarization of the photoelectrons from the TSSs is 100%, the measured value will always be lower than this due, e. g., to spin-unpolarized background signals and finite resolution of the apparatus.

Equation (2) and our discussion based on it are not confined to topological insulators and can provide a guidance for the interpretation of any spin-resolved photoemission experiment using fully-polarized light.

So far, we have discussed the magnitude of the spin polarization, without resorting to the details of the system. Now, by obtaining the state $|f'\rangle$ in Eq. (3) using the specific symmetries of the TI surface, we determine the orientation of the spin polarization. We adopt the commonly used effective Hamiltonian $H_{\text{TI}}^0(\mathbf{k})$ for the Bloch periodic part $|\phi(n, \mathbf{k})\rangle$ of the wavefunction of TSSs in a TI with (in-plane) Bloch wavevector $\mathbf{k} = k_x \hat{x} + k_y \hat{y}$ (\hat{z} is along the surface normal) given by

$$H_{\text{TI}}^0(\mathbf{k}) = \hbar v k (\sin \theta_{\mathbf{k}} \sigma_x - \cos \theta_{\mathbf{k}} \sigma_y), \quad (6)$$

where v is the band velocity, $\theta_{\mathbf{k}}$ the angle between \mathbf{k} and the $+k_x$ direction, and σ_x and σ_y are the Pauli matrices acting on a two-component wavefunction, the so-called pseudospins. In constructing the effective Hamiltonian in Eq. (6), the basis states defining the $\begin{pmatrix} 1 \\ 0 \end{pmatrix}$ and $\begin{pmatrix} 0 \\ 1 \end{pmatrix}$ column vectors, corresponding to pseudospin up and down states, are constructed from the two degenerate states at $\mathbf{k} = 0$.

Here, we consider a class of materials having the symmetry of the surface of Bi_2Se_3 or Bi_2Te_3 ; however, the development can straightforwardly be extended to other classes. The two states at $\mathbf{k} = 0$ which are used as basis, $|\phi_1\rangle$ and $|\phi_2\rangle$, can then be uniquely fixed by using the

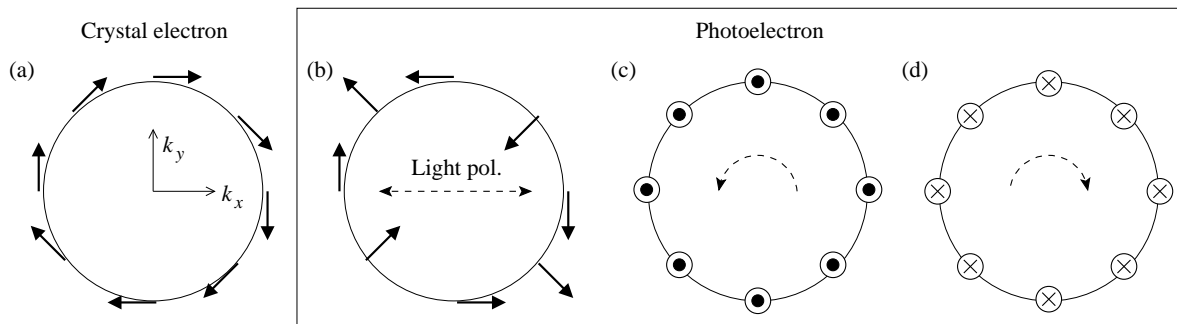


FIG. 1: (a) The spin orientation of the surface states in a topological insulator on an equi-energy contour in the upper band [$n = +1$ in Eqs. (8) and (9)]. (b)-(d): Similar quantities as in (a) for the measured photoelectrons with light having linear (along the $+x$ direction), left-handed circular, and right-handed circular polarizations, respectively. (For the latter two, the handedness is defined from the viewpoint of the light source.) The surface normal direction is \hat{z} .

symmetry properties:

$$\begin{aligned} \Theta |\phi_1\rangle &= -|\phi_2\rangle, & \Theta |\phi_2\rangle &= |\phi_1\rangle, \\ M |\phi_1\rangle &= i|\phi_2\rangle, & M |\phi_2\rangle &= i|\phi_1\rangle, \\ C_3 |\phi_1\rangle &= e^{-i\pi/3} |\phi_1\rangle, & C_3 |\phi_2\rangle &= e^{+i\pi/3} |\phi_2\rangle, \end{aligned} \quad (7)$$

where Θ is the time-reversal operator, M the reflection operator, $x \rightarrow -x$ (\hat{x} is along the ΓK direction), and C_3 the operator for $2\pi/3$ rotation around the z axis. The eigenvalue and Bloch periodic eigenstate are

$$E(n, \mathbf{k}) = n \hbar v k, \quad (8)$$

and

$$|\phi(n, \mathbf{k})\rangle = \frac{1}{\sqrt{2}} (|\phi_1\rangle - n i e^{i\theta_{\mathbf{k}}} |\phi_2\rangle) = \begin{pmatrix} 1 \\ -n i e^{i\theta_{\mathbf{k}}} \end{pmatrix}, \quad (9)$$

respectively, where $n = \pm 1$ is the band index. The pseudospin expectation value of the TSS [Eq. (9)] is thus given by

$$\langle \vec{\sigma} \rangle = n (\sin \theta_{\mathbf{k}} \hat{x} - \cos \theta_{\mathbf{k}} \hat{y}). \quad (10)$$

It is known that the actual spin expectation value $\langle \mathbf{s} \rangle$ is aligned with the pseudospin expectation value [7], i. e. ,

$$\langle \mathbf{s} \rangle \propto n (\sin \theta_{\mathbf{k}} \hat{x} - \cos \theta_{\mathbf{k}} \hat{y}). \quad (11)$$

The orientation of the spinor eigenstates in the upper band ($n = +1$) is shown in Fig. 1(a).

In calculating photoemission matrix elements, we use the theoretical framework of Wang *et al.* [15]. At small \mathbf{k} , it is assumed that the final photoemission states $|f\rangle$'s are spin-degenerate because they are well within the spin-degenerate bulk band continuum. In matrix element calculations for small \mathbf{k} , we will approximate the periodic part of the final state Bloch wavefunctions $|\phi_{\uparrow}^f(\mathbf{k}, k_{\perp})\rangle$ and $|\phi_{\downarrow}^f(\mathbf{k}, k_{\perp})\rangle$ by those with $\mathbf{k} = 0$ and

$k_{\perp} = \sqrt{\frac{2m_e}{\hbar^2}(h\nu - E_D)}$, where k_{\perp} is the surface normal component of the photoelectron wavevector, m_e the electron mass and E_D the energy of two-fold degenerate TSSs at $\mathbf{k} = 0$. We denote these two (\mathbf{k} -independent) states by $|\phi_{\uparrow}^f\rangle$ and $|\phi_{\downarrow}^f\rangle$, respectively, and use the same symmetry relations as in Eq. (7) to define these states. Also, we will neglect the momentum dependence of the velocity operator $\mathbf{v}(\mathbf{k}) = e^{-i\mathbf{r}\cdot\mathbf{k}} \mathbf{v} e^{i\mathbf{r}\cdot\mathbf{k}}$ [see Eq. (14)]. that has to be used in calculating the optical transition matrix element between the periodic parts of the Bloch wavefunctions. This theoretical setup [15] was employed to find the energy- and momentum-dependent spin polarization of the TSS in Bi_2Se_3 from time-of-flight ARPES measurement with laser of energy 6.2 eV. The spin polarization of TSS electrons thus obtained is in excellent agreement with theory [20] and other spin-resolved ARPES experiments [8, 10–12]. Therefore, our theoretical development and predictions below should be valid when low-energy light source is employed.

An important point to note here is that $|\phi_{\uparrow}^f\rangle$ and $|\phi_{\downarrow}^f\rangle$ are the actual spin-up and spin-down states along \hat{z} far away from the surface in vacuum where the measurement is performed, because we have imposed the symmetry constraints of the system in Eq. (7) [5, 20]. Even though the real spin character of those two basis states at the surface can be very complicated, we can regard the chosen degenerate doublet $|\phi_{\uparrow}^f\rangle$ and $|\phi_{\downarrow}^f\rangle$ the actual spin-up and spin-down states, respectively, from a measurement point of view.

Next, the microscopic Hamiltonian H_D of an electron with spin-orbit coupling [21] is given by

$$H_D = \frac{\mathbf{p}^2}{2m_e} + V + \frac{\hbar}{4m_e^2 c^2} (\nabla V \times \mathbf{p}) \cdot \mathbf{s}, \quad (12)$$

where V is the one-electron potential. Using Peierls substitution $\mathbf{p} \rightarrow \mathbf{p} - \frac{e}{c} \mathbf{A}$, where \mathbf{A} is the vector potential

of the electromagnetic wave, and the relation $H_D^{\text{int}}(\mathbf{A}) = H_D(\mathbf{p} - \frac{e}{\hbar c}\mathbf{A}) - H_D(\mathbf{p})$, we obtain the electron-photon interaction Hamiltonian

$$H_D^{\text{int}}(\mathbf{A}) = -\frac{e}{c}\mathbf{A} \cdot \mathbf{v}, \quad (13)$$

where

$$\mathbf{v} = \frac{\mathbf{p}}{m_e} + \frac{\hbar}{4m_e^2c^2}(\mathbf{s} \times \nabla V) \quad (14)$$

is the velocity operator [21].

We first consider the matrix elements

$$\mathbf{v}_{s,i} = \langle \phi_s^f | \mathbf{v} | \phi_i \rangle, \quad (15)$$

where $s = \uparrow$ or \downarrow and $i = 1$ or 2 are the index of the photo-excite state and the pseudospin basis index of the TSS state, respectively. If we define

$$v_{\pm} = v_x \pm i v_y \quad (16)$$

and use the symmetry of the system for both the initial and final states [Eq. (7)], only the following four are non-zero among twelve possible combinations [15]:

$$\begin{aligned} \langle \phi_{\uparrow}^f | v_+ | \phi_2 \rangle &= \langle \phi_{\downarrow}^f | v_- | \phi_1 \rangle^* = i\alpha \\ \langle \phi_{\uparrow}^f | v_z | \phi_1 \rangle &= \langle \phi_{\downarrow}^f | v_z | \phi_2 \rangle = i\beta, \end{aligned} \quad (17)$$

where α and β are *real* constants which can be determined from, e. g., first-principles calculations.

Plugging Eqs. (15) and (17) into Eq. (13), we obtain the interaction Hamiltonian matrix $H_{\text{TI}}^{\text{int}}(\mathbf{A})$ connecting the two basis functions of the TSSs, $|\phi_1\rangle$ and $|\phi_2\rangle$, to the spin-up and spin-down photoexcited states, $|\phi_{\uparrow}^f\rangle$ and $|\phi_{\downarrow}^f\rangle$:

$$H_{\text{TI}}^{\text{int}}(\mathbf{A}) = \frac{\alpha}{2c} e \left[(A_y \sigma_x - A_x \sigma_y) + i \left(\frac{2\beta}{\alpha} \right) A_z I \right], \quad (18)$$

where I is the 2×2 identity matrix. In this study, we neglect the last term that depends on the z component of the light polarization, i. e., we set $A_z = 0$, in order to see the new physics clearly. Because this term is proportional to the identity matrix, it alone does not contribute to alteration of the spin direction of a photoemitted electron from that of the initial state.

First we consider the case where the light is linearly polarized. Then,

$$H_{\text{TI}}^{\text{int}}(\mathbf{A}) = \frac{\alpha}{2c} eA (\sin \theta_{\mathbf{A}} \sigma_x - \cos \theta_{\mathbf{A}} \sigma_y), \quad (19)$$

where $\theta_{\mathbf{A}}$ is the angle between the vector potential \mathbf{A} and the $+x$ direction. As we discussed before, the photocurrent is given by Eq. (2), where in our case $|i\rangle = |\phi(n, \mathbf{k})\rangle$

[Eq. (9)] and $|f\rangle$'s are $|\phi_{\uparrow}^f\rangle$ and $|\phi_{\downarrow}^f\rangle$. Since the photocurrent $I_{\hat{t}}$ is nothing but the squared projection of the state $|f\rangle$ in Eq. (3) to the detector state $|\hat{t}, \mathbf{R}_D\rangle$, it is essential to know the spin orientation of $|f\rangle$. Using Eq. (19), we can write $|f\rangle$ [Eq. (3)] in the basis of $|\phi_{\uparrow}^f\rangle$ and $|\phi_{\downarrow}^f\rangle$ as

$$|\phi'(n, \mathbf{k})\rangle = \frac{1}{\sqrt{2}} \begin{pmatrix} 1 \\ -ni e^{i(2\theta_{\mathbf{A}} - \theta_{\mathbf{k}})} \end{pmatrix}. \quad (20)$$

Comparing Eqs. (9) with (20) and using Eqs. (10) and (11), we find that the net effect of photoexcitation on the detected electron spin polarization direction defined by the direction \hat{t} maximizing $(I_{\hat{t}} - I_{-\hat{t}})/(I_{\hat{t}} + I_{-\hat{t}})$ in Eq. (1) is a rotation in direction through a change

$$\theta_{\mathbf{k}} \rightarrow \theta_{\mathbf{k}} + 2\Delta\theta_{\mathbf{A},\mathbf{k}}, \quad (21)$$

where $\Delta\theta_{\mathbf{A},\mathbf{k}} \equiv \theta_{\mathbf{A}} - \theta_{\mathbf{k}}$ is the angle between the in-plane light polarization and the Bloch wavevector. The spin expectation value of the photoelectron arriving at the detector $\langle \mathbf{s} \rangle_f$ in units of $\hbar/2$ is thus given by

$$\langle \mathbf{s} \rangle_f = n [\sin(\theta_{\mathbf{k}} + 2\Delta\theta_{\mathbf{A},\mathbf{k}}) \hat{x} - \cos(\theta_{\mathbf{k}} + 2\Delta\theta_{\mathbf{A},\mathbf{k}}) \hat{y}]. \quad (22)$$

(Note that the magnitude of the spin polarization is 100% in agreement with the above, general discussion.)

For the special case of $\theta_{\mathbf{k}} = \theta_{\mathbf{A}}$, the spin orientation of the photoelectron [Eq. (22)] is the same as that of the initial TSS electron [Eq. (11)]. However, in general, the two are different. Especially, for states whose Bloch wavevector \mathbf{k} is perpendicular to the in-plane component of the light polarization \mathbf{A} [i. e., $|\Delta\theta_{\mathbf{A},\mathbf{k}}| = \pi/2$ in Eq. (21)], the initial and final spins are *antiparallel* to each other.

For in-plane circularly polarized light, the vector potential is given by $\mathbf{A} = A(\hat{x} \pm i\hat{y})/\sqrt{2}$ with the $+$ and $-$ signs denoting left-handed and right-handed circular polarizations as defined from the viewpoint of the light source, respectively. Then, within the effective Hamiltonian formalism [Eq. (18)],

$$H_{\text{TI}}^{\text{int}}(\mathbf{A}) = \frac{\alpha}{2\sqrt{2}c} eA (\pm i \sigma_x - \sigma_y). \quad (23)$$

Applying the same argument as before, the spin polarization direction of the photoelectron measured by a spin-resolved detector is that of

$$|\phi'(n, \mathbf{k})\rangle_{\text{LHC}} = \begin{pmatrix} 1 \\ 0 \end{pmatrix} = |\phi_{\uparrow}^f\rangle \quad (24)$$

and

$$|\phi'(n, \mathbf{k})\rangle_{\text{RHC}} = \begin{pmatrix} 0 \\ 1 \end{pmatrix} = |\phi_{\downarrow}^f\rangle, \quad (25)$$

for left-handed and right-handed circular polarizations, respectively. The spin polarization direction of the pho-

toelectrons are thus pointed along the parallel ($+\hat{z}$) and antiparallel ($-\hat{z}$) directions to the surface normal, for left-handed [Fig. 1(c)] and right-handed [Fig. 1(d)] circular polarized light, respectively.

The phenomenon of photo-induced spin rotation in a TI predicted here was not observed previously. The reason is that $\Delta\theta_{\mathbf{A},\mathbf{k}}$ in Eq. (22) was held fixed or was allowed to change little in conventional spin-resolved ARPES measurements by linearly polarized light as different \mathbf{k} states were probed. Recently, Lanzara and coworkers [22] have tuned $\Delta\theta_{\mathbf{A},\mathbf{k}}$ and confirmed the photo-induced spin rotations, as predicted here for both linearly [Eq. (22)] and circularly [Eqs. (24) and (25)] polarized lights.

In conclusion, we have shown that in spin-resolved photoemission experiments, the measured degree of spin polarization of photoelectrons with a specific energy is 100% under ideal condition regardless of that of the initial state if the initial state is not degenerate and fully-polarized light is used. We have used this general principle to explain why the degree of spin polarization of the photoelectrons from the surface states of a topological insulator can be higher than that of the initial states. Using the specific symmetries of the system, we have further shown that the spin polarization direction of photoexcited electrons from the topological surface states is in general very different from that of the initial states and is dictated by the light polarization. Our results provide a theoretical basis for manipulation of the spin polarization of the photoelectrons from the topological surface states [22–24].

We thank A. Lanzara, C. Jozwiak, C. Hwang and J. D. Sau for discussions. Theoretical part of this work was supported by National Science Foundation Grant No. DMR10-1006184 and simulations part by the Director, Office of Science, Office of Basic Energy Sciences, Materials Sciences and Engineering Division, U.S. Department of Energy under Contract No. DE-AC02-05CH11231.

* Electronic address: sglouie@berkeley.edu

- [1] L. Fu, C. L. Kane, and E. J. Mele, Phys. Rev. Lett. **98**, 106803 (2007).
- [2] J. E. Moore and L. Balents, Phys. Rev. B **75**, 121306 (2007).
- [3] R. Roy, Phys. Rev. B **79**, 195322 (2009).
- [4] D. Hsieh *et al.*, Nature **452**, 970 (2008).
- [5] H. Zhang *et al.*, Nature Phys. **5**, 438 (2009).
- [6] O. V. Yazyev, J. E. Moore, and S. G. Louie, Phys. Rev. Lett. **105**, 266806 (2010).
- [7] M. Z. Hasan and C. L. Kane, Rev. Mod. Phys. **82**, 3045 (2010).
- [8] D. Hsieh *et al.*, Science **323**, 919 (2009).
- [9] D. Hsieh *et al.*, Nature **460**, 1101 (2009).
- [10] S. Souma *et al.*, Phys. Rev. Lett. **106**, 216803 (2011).
- [11] S.-Y. Xu *et al.*, arXiv:1101.3985.

- [12] Z.-H. Pan *et al.*, Phys. Rev. Lett. **106**, 257004 (2011).
- [13] C. Jozwiak *et al.*, Phys. Rev. B **84**, 165113 (2011).
- [14] Y. Ishida *et al.*, Phys. Rev. Lett. **107**, 077601 (2011).
- [15] Y. H. Wang *et al.*, Phys. Rev. Lett. **107**, 207602 (2011).
- [16] S. R. Park *et al.*, Phys. Rev. Lett. **108**, 046805 (2012).
- [17] M. R. Scholz *et al.*, arXiv:1108.1053.
- [18] Supplementary material.
- [19] *The Feynman Lectures on Physics*, edited by R. P. Feynman, R. B. Leighton, and M. Sands (Addison-Wesley, Boston, 1964), Vol. 3.
- [20] L. Fu, Phys. Rev. Lett. **103**, 266801 (2009).
- [21] G. Dresselhaus, Phys. Rev. **100**, 580 (1955).
- [22] C. Jozwiak *et al.*, submitted.
- [23] W.-K. Tse and A. H. MacDonald, Phys. Rev. Lett. **105**, 057401 (2010).
- [24] J. W. McIver *et al.*, Nat. Nanotechnol. **7**, 96 (2012).

SUPPLEMENTAL MATERIAL

1. Fermi's golden rule

Consider an electronic system described by a single-particle Hamiltonian H_0 with energy eigenvalues and corresponding eigenstates E_n and $|n\rangle$, respectively, where n is the state index. Suppose now that we have a time-dependent perturbation of the form $H^{\text{int}}(t) = H^{\text{int}}(\mathbf{A}) e^{-2\pi i\nu t}$, where \mathbf{A} is the vector potential and $h\nu$ the photon energy, in addition to the original Hamiltonian H_0 . The total Hamiltonian is given by

$$H(t) = H_0 + H^{\text{int}}(\mathbf{A}) e^{-2\pi i\nu t}. \quad (26)$$

We are interested in the evolution of an electron which is at $|i\rangle$ before turning on the time-dependent perturbation. Assuming that the perturbation is turned on at $t = 0$, the wavefunction satisfying normalization condition ($\langle\psi(t)|\psi(t)\rangle = 1$) to first order can be written as

$$|\psi(t)\rangle = e^{-iE_i t/\hbar} |i\rangle + \sum_f c_f(t) e^{-iE_f t/\hbar} |f\rangle, \quad (27)$$

where $c_f(t)$ is the probability amplitude of finding an electron in state $|f\rangle$ at a given time t . Obviously,

$$c_f(0) = 0. \quad (28)$$

Using Eqs. (26), (27), and (28), we can solve the time-dependent Schrödinger equation and arrive at

$$c_f(t) = -i e^{it} \frac{\Delta E_f}{2\hbar} \frac{\sin t \frac{\Delta E_f}{2\hbar}}{\frac{\Delta E_f}{2}} \langle f | H^{\text{int}} | i \rangle, \quad (29)$$

where

$$\Delta E_f \equiv (E_f - E_i) - h\nu. \quad (30)$$

Equation (29) leads to

$$P_f(t) \equiv |c_f(t)|^2 = \frac{t}{\hbar^2} \frac{\sin^2 t \frac{\Delta E_f}{2\hbar}}{\left(\frac{\Delta E_f}{2\hbar}\right)^2} |\langle f | H^{\text{int}} | i \rangle|^2. \quad (31)$$

Using the following relation

$$\lim_{a \rightarrow \infty} \frac{1}{\pi} \frac{\sin^2(ax)}{ax^2} = \delta(x), \quad (32)$$

we finally obtain

$$\begin{aligned} \Gamma_{f \leftarrow i} &= \lim_{t \rightarrow \infty} P_f(t)/t \\ &= \frac{\pi}{\hbar^2} \delta\left(\frac{\Delta E_f}{2\hbar}\right) |\langle f | H^{\text{int}} | i \rangle|^2 \\ &= \frac{2\pi}{\hbar} \delta(\Delta E_f) |\langle f | H^{\text{int}} | i \rangle|^2, \end{aligned} \quad (33)$$

which is Fermi's golden rule.

2. Spin-resolved photoemission experiment

Now we find an expression for photocurrent $I_{\hat{t}}$ in spin-resolved photoemission experiment with a detector aligned such that it captures electrons in a state $|\hat{t}, \mathbf{R}_D\rangle$ of which (i) the spin part is the eigenvector of $\mathbf{s} \cdot \hat{t}$ with eigenvalue +1 and (ii) the spatial part is localized at the detector ($\mathbf{r} = \mathbf{R}_D$) as in the main manuscript. The photocurrent is then given by

$$I_{\hat{t}} \propto \lim_{t \rightarrow \infty} \left| \langle \hat{t}, \mathbf{R}_D | \psi(t) \rangle \right|^2 / t. \quad (34)$$

Note that in the previous section, we have used $|f\rangle$ in the place of $|\hat{t}, \mathbf{R}_D\rangle$ to derive Fermi's golden rule; replacement of the final state is the only difference.

Using Eqs. (27) and (29), we can write $\langle \hat{t}, \mathbf{R}_D | \psi(t) \rangle$ as

$$\begin{aligned} \langle \hat{t}, \mathbf{R}_D | \psi(t) \rangle &= \sum_E \sum_{\{f|E_f=E\}} -i e^{it} \frac{\Delta E_f}{2\hbar} \frac{\sin t \frac{\Delta E_f}{2\hbar}}{\frac{\Delta E_f}{2}} \langle f | H^{\text{int}} | i \rangle e^{-iE_f t/\hbar} \langle \hat{t}, \mathbf{R}_D | f \rangle \\ &= \sum_E -i e^{it} \frac{\Delta E - 2E}{2\hbar} \frac{\sin t \frac{\Delta E}{2\hbar}}{\frac{\Delta E}{2}} \sum_{\{f|E_f=E\}} \langle \hat{t}, \mathbf{R}_D | f \rangle \langle f | H^{\text{int}} | i \rangle, \end{aligned} \quad (35)$$

where $\Delta E = (E - E_i) - h\nu$. An important knowledge we made use of in Eq. (35) is that $\langle \hat{t}, \mathbf{R}_D | i \rangle = 0$ because

the initial state is localized at the crystal and does not extend to the detector. Obviously, a product of the terms in Eq. (35) corresponding to different E values does not contribute to the photocurrent calculated from Eq. (34). Plugging Eq. (35) into Eq. (34) and using Eq. (32) again, we obtain the expression for the photocurrent:

$$\begin{aligned} I_{\hat{t}} &\propto \sum_E \delta(E - E_i - h\nu) \left| \sum_{\{f|E_f=E\}} \langle \hat{t}, \mathbf{R}_D | f \rangle \langle f | H^{\text{int}} | i \rangle \right|^2 \\ &\propto \left| \sum_{\{f|E_f=E_i+h\nu\}} \langle \hat{t}, \mathbf{R}_D | f \rangle \langle f | H^{\text{int}} | i \rangle \right|^2, \end{aligned} \quad (36)$$

which is Eq. (2) of the main manuscript. Equivalently,

Eq. (36) can also be written as

$$I_{\hat{t}} \propto \left| \sum_f \delta(E_f - E_i - h\nu) \langle \hat{t}, \mathbf{R}_D | f \rangle \langle f | H^{\text{int}} | i \rangle \right|^2. \quad (37)$$